Automatica 46 (2010) 29–39

Contents lists available at ScienceDirect

Automatica

journal homepage: www.elsevier.com/locate/automatica

An integral predictive/nonlinear $\mathcal{H}_\infty$ control structure for a quadrotor helicopter☆

Guilherme V. Raffo *, Manuel G. Ortega, Francisco R. Rubio

Departamento de Ingeniería de Sistemas y Automática, Universidad de Sevilla, Camino de los Descubrimientos s/n, 41092, Sevilla, Spain

ARTICLE INFO

Article history:
Received 2 March 2009
Received in revised form
21 September 2009
Accepted 29 September 2009
Available online 13 November 2009

Keywords:
Nonlinear $\mathcal{H}_\infty$ control
Predictive control
Robust control
Unmanned aerial vehicle

ABSTRACT

This paper presents an integral predictive and nonlinear robust control strategy to solve the path following problem for a quadrotor helicopter. The dynamic motion equations are obtained by the Lagrange–Euler formalism. The proposed control structure is a hierarchical scheme consisting of a model predictive controller (MPC) to track the reference trajectory together with a nonlinear $\mathcal{H}_\infty$ controller to stabilize the rotational movements. In both controllers the integral of the position error is considered, allowing the achievement of a null steady-state error when sustained disturbances are acting on the system. Simulation results in the presence of aerodynamic disturbances, parametric and structural uncertainties are presented to corroborate the effectiveness and the robustness of the proposed strategy.

1. Introduction

The development of unmanned aerial vehicles (UAV's) have generated great interest in the automatic control area in the last few decades. These kinds of vehicles have been used in tasks such as search and rescue, building exploration, security and inspection. The UAV's are most useful, mainly, when these desired tasks are executed in dangerous and inaccessible environments.

In the last few years the UAV in the quadrotor configuration has been highlighted in a lot of papers. This vehicle is based on VTOL (Vertical Take-Off and Landing) concepts and it is usually used to develop control laws. This kind of helicopter tries to reach a stable hovering and flight using the equilibrium forces produced by four rotors (Castillo, Lozano, & Dzul, 2005b). One of the advantages of the quadrotor configuration is its load capacity. Moreover, this helicopter is highly maneuverable, which allows take-off and landing as well as flight in tough environment. One drawback, is that this type of UAV presents a weight and energy consumption augmentation due to the extra motors.

Nevertheless, these kinds of UAV's have a high nonlinear and time-varying behavior and they are constantly affected by aerodynamic disturbances. In addition, UAV's are usually models subject to unmodelled dynamics and parametric uncertainties. Therefore, an advanced control strategy is required to achieve good performance in autonomous flight or at least to help the piloting of the vehicle, with high maneuverability and robustness with respect to external disturbances.

Concerning this matter, it must be taken into account that these vehicles are underactuated mechanical systems, which complicate the control design stage even more. Techniques developed for fully actuated robots cannot be directly applied to this class of systems (Fantoni & Lozano, 2002). Therefore, nonlinear modelling techniques and modern nonlinear control theory are usually employed to achieve autonomous flight with high performance (Castillo et al., 2005b).

Many efforts have been made to control quadrotor-based helicopters and some strategies have been developed to solve the path following problems for this type of system. In Mistler, Benallegue, and M'Sirdi (2001), the aerodynamic forces and moments acting on this model were considered. The path following problem was solved using exact linearization techniques and noninteracting control via dynamic feedback. In Bouabdallah, Murrieri, and Siegwart (2004) the rotor dynamics were considered in the model. The model was split up into two subsystems: the angular rotations and the linear translations. Backstepping and sliding mode techniques were used to control the helicopter. In Raffo, Ortega, and Rubio (2008) a control law based on a standard backstepping approach for translational movements and a nonlinear $\mathcal{H}_\infty$ controller to stabilize the helicopter are combined to perform path following in the presence of external disturbances and parametric uncertainties. However, this strategy is only able to reject sustained disturbances applied to the rotational motion. In several publications the backstepping technique was used to perform

☆ This paper was not presented at any IFAC meeting. This paper was recommended for publication in revised form by Associate Editor Warren E. Dixon under the direction of Editor Andrew R. Teel.

* Corresponding author. Tel.: +34 95 448 7487; fax: +34 95 448 7340.
E-mail address: raffo@cartuja.us.es (G.V. Raffo).

0005-1098/$ – see front matter © 2009 Elsevier Ltd. All rights reserved.
doi:10.1016/j.automatica.2009.10.018

both path following and stabilization problems. Backstepping approaches applied to the quadrotor helicopter are found in Madani and Benallegue (2007), Zemalache, Beji, and Maaref (2007) and Guenard, Hamel, and Mahony (2008).

However, most of the control strategies tested on the quadrotor helicopter do not consider external disturbances on the six degrees of freedom and parametric uncertainties of the model. In the last few years researchers have begun to consider these effects at the control law design stage. In Mokhtari, Benallegue, and Orlov (2006) a feedback linearization-based controller with a sliding mode observer was designed for the quadrotor helicopter. An adaptive observer was added to the control system to estimate the effect of external disturbances. In Bouabdallah and Siegwart (2007) a backstepping approach using integral action was used to improve the quadrotor helicopter path following performance when maintained winds disturb whole the system.

In some papers the quadrotor helicopter has also been controlled using a linear $\mathcal{H}_\infty$ controller based on linearized models. In Chen and Huzmezan (2003), a simplified nonlinear model of the UAV movements was presented. The path following problem was divided into two parts, the first one to achieve the angular rates and vertical velocity stabilization by a 2DOF linear $\mathcal{H}_\infty$ controller using the loop shaping technique. The same technique was used to control the longitudinal and lateral velocities, the yaw angle and the height in the outer loop. In the second part a predictive control was designed to solve the path following problem. In Mokhtari, Benallegue, and Daachi (2006) a robust feedback linearization with a linear $\mathcal{H}_\infty$ controller was applied to deal with the path following problem with parameter uncertainties and external disturbances.

Furthermore, there are two issues that are worth pointing out. On one hand, most of the above control applications assume that the computed control actions will never reach the saturation limits of the actuators, although in practice it is possible. For instance, when the UAV is far away from its destination, the generated control signals are normally higher than the admissible values. Moreover, the vehicles are composed of mechanical and electrical parts, which are also subject to physical constraints.

When on-line constraints must be considered, model predictive controller (MPC) algorithms appear as an interesting choice. The objective of MPC is to compute a future control sequence in a defined horizon in such a way that the prediction of the plant output is driven close to the reference. This is accomplished by minimizing a multistage cost function with respect to the future control actions. An analytical solution can be obtained for a quadratic cost function if the model is linear and there are no constraints; otherwise an iterative method of optimization should be used (Camacho & Bordons, 1998). Moreover, the MPC formulation generates (implicitly) a nonsmooth control law. Given that trajectories are normally known and using an appropriate vehicle instrumentation to inform about position, orientation and movements (e.g. using a GPS, digital maps, etc.), the predictive controller becomes even more suitable for this task. Apart from the fact that MPC guides the system smoothly, it presents an enhanced autonomy and can easily be extended to multivariable systems.

On the other hand, UAV's are constantly affected by model uncertainties and wind gusts, which can easily destabilize the vehicle. A good choice to reject these disturbances is the nonlinear $\mathcal{H}_\infty$ control theory. The goal of this control theory, presented by Van der Schaft in Van der Schaft (1992), is to achieve a bounded ratio between the energy of the so-called error signals and the energy of the disturbance signals. In general, the nonlinear approach of this theory considers two Hamilton–Jacobi–Bellman–Isaacs partial differential equations (HJBI PDEs), which replace the Riccati equations in the case of the linear $\mathcal{H}_\infty$ control formulation. The main problem in the nonlinear case is the absence of a general method to solve these HJBI PDEs.

In this paper, an integral predictive and nonlinear robust control strategy to solve the path following problem of the quadrotor helicopter is proposed. The main idea is to combine the advantages of the predictive control methodology to follow a predefined trajectory in a smooth way, with the capacity of the nonlinear $\mathcal{H}_\infty$ theory to cope with unknown disturbances. To carry out these objectives, a state-space predictive controller with integral action based on the time variant error model is used to track the reference trajectory, which is an improvement of the controller presented in Raffo, Gomes, Normey-Rico, Kelber, and Becker (2009). To stabilize the helicopter rotational movements a nonlinear $\mathcal{H}_\infty$ controller is synthesized. Both controllers consider the position error integral that allows the sustained disturbances rejection.

The nonlinear $\mathcal{H}_\infty$ approach used in this paper consists in an adaptation of a previous work, presented in Ortega, Vargas, Vivas, and Rubio (2005), formulated via game theory, to control mechanical systems considering the tracking error dynamic equation. This strategy provides, through an analytical solution, a time variant control law which is strongly model-dependent and it is similar to the results obtained with the feedback linearization procedures.

The remainder of the paper is organized as follows: in Section 2, a description of the quadrotor helicopter model is given. The control strategy is exposed in Section 3. In Section 4 the nonlinear $\mathcal{H}_\infty$ controller for the rotational subsystem is developed. The predictive controller for the translational movements is presented in Section 5. Simulation results are presented in Section 6. Finally, the major conclusions of the paper are drawn in Section 7.

2. System modelling

2.1. Description

The autonomous aerial vehicle used in this paper is a miniature four rotor helicopter. The movement of the UAV results from changes on the lift force caused by adjusting the velocities of the rotors. Longitudinal motions are achieved by means of front and rear rotors velocity, changing the forces f_1 and f_3 (see Fig. 1), while lateral displacements are performed through the speed of the right and left propellers, which causes a variation on forces f_2 and f_4. Yaw movements are obtained from the difference in the counter-torque between each pair of propellers, (f_1, f_3) and (f_2, f_4), i.e., accelerating the two clockwise turning rotors while decelerating the counter-clockwise turning rotors, and vice versa. Finally, the total thrust, which displaces the helicopter in the perpendicular plane with respect to the propellers, is obtained by the sum of the four forces generated by propellers.

This kind of system is a flight vehicle of lightweight structure and, therefore, gyroscopic effects resulting from the rotation of the rigid body and the four propellers should be included in the dynamic model (Bouabdallah, Noth, & Siegwart, 2004). However, in this paper the dynamic model of the system is obtained under the assumption that the vehicle is a rigid body in the space subject to one main force (thrust) and three torques. This simplification implies that gyroscopic effects caused by the propellers will be considered as disturbances for the rotational control law.

Besides, this helicopter is an underactuated mechanical system with six degrees of freedom and only four control inputs. Due to the complexities presented, some assumptions are made to compute the model for control purposes. The ground effect is neglected and the center of mass and the body fixed frame origin are assumed congruent. Moreover, for controller synthesis purposes, the helicopter structure is assumed to be symmetric, which results in a moment of inertia tensor with just diagonal inertia terms.

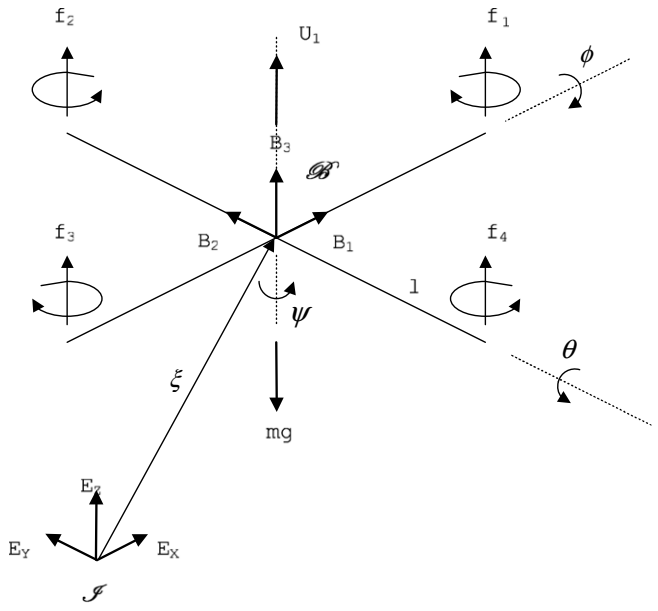

Fig. 1. Quadrotor helicopter scheme.

2.2. Helicopter kinematics

The helicopter as a rigid body is characterized by a frame linked to it. Let $\mathscr{B} = \{B_1, B_2, B_3\}$ be the body fixed frame, where the B_1 axis is in the helicopter normal flight direction, B_2 is orthogonal to B_1 and positive to starboard in the horizontal plane, whereas B_3 is oriented in the ascendant sense and orthogonal to the plane B_1OB_2. The inertial frame $\mathscr{I} = \{E_x, E_y, E_z\}$ is considered fixed with respect to the earth (see Fig. 1).

The vector $\boldsymbol{\xi} = [x \quad y \quad z]'$ represents the position of the helicopter mass center expressed in the inertial frame $\mathscr{I}$.[1] The vehicle orientation is given by a rotation matrix $\boldsymbol{R}_{\mathscr{I}} : \mathscr{B} \to \mathscr{I}$, where $\boldsymbol{R}_{\mathscr{I}} \in SO(3)$ is an orthonormal rotation matrix (Fantoni & Lozano, 2002). The rotation matrix can be obtained through three successive rotations around the axes of the body fixed frame. In this paper, the *XYZ* fixed Euler angles have been used to describe the helicopter rotation with respect to the ground. These angles are bounded as follows: roll angle, ϕ, by $(-\pi/2 < \phi < \pi/2)$; pitch angle, θ, by $(-\pi/2 < \theta < \pi/2)$; and yaw angle, ψ, by $(-\pi < \psi < \pi)$.

From these three rotations, the following rotation matrix from $\mathscr{B}$ to $\mathscr{I}$ is obtained:

$$\boldsymbol{R}_{\mathscr{I}} = \begin{bmatrix} C\psi C\theta & C\psi S\theta S\phi - S\psi C\phi & C\psi S\theta C\phi + S\psi S\phi \\ S\psi C\theta & S\psi S\theta S\phi + C\psi C\phi & S\psi S\theta C\phi - C\psi S\phi \\ -S\theta & C\theta S\phi & C\theta C\phi \end{bmatrix} \tag{1}$$

where $C\cdot = \cos(\cdot)$ and $S\cdot = \sin(\cdot)$.

The kinematic equations of the rotational and translational movements are obtained by means of the rotation matrix. The translational kinematic can be written as:

$$\boldsymbol{v}_{\mathscr{I}} = \boldsymbol{R}_{\mathscr{I}} \cdot \boldsymbol{v}_{\mathscr{B}} \tag{2}$$

where $\boldsymbol{v}_{\mathscr{I}} = [u_0 \quad v_0 \quad w_0]'$ and $\boldsymbol{v}_{\mathscr{B}} = [u_L \quad v_L \quad w_L]'$ are linear velocities of the mass center expressed in the inertial frame and body fixed frame, respectively.

The rotational kinematics can be obtained from the relationship between the rotation matrix and its derivative with a skew-symmetric matrix (Craig, 1989; Olfati-Saber, 2001) as follows:

$$\dot{\boldsymbol{\eta}} = \boldsymbol{W}_{\eta}^{-1}\boldsymbol{\omega}$$

$$\begin{bmatrix} \dot{\phi} \\ \dot{\theta} \\ \dot{\psi} \end{bmatrix} = \begin{bmatrix} 1 & \sin\phi\tan\theta & \cos\phi\tan\theta \\ 0 & \cos\phi & -\sin\phi \\ 0 & \sin\phi\sec\theta & \cos\phi\sec\theta \end{bmatrix} \begin{bmatrix} p \\ q \\ r \end{bmatrix} \tag{3}$$

where $\boldsymbol{\eta} = [\phi \quad \theta \quad \psi]'$, and $\boldsymbol{\omega} = [p \quad q \quad r]'$ are the angular velocities in the body fixed frame.

2.3. Lagrange–Euler equations

The helicopter motion equations can be expressed by the Lagrange–Euler formalism based on the kinetic and potential energy concept:

$$\begin{bmatrix} \boldsymbol{f}_{\xi} \\ \boldsymbol{\tau}_{\eta} \end{bmatrix} = \frac{\mathrm{d}}{\mathrm{d}t}\left(\frac{\partial L}{\partial \dot{q}_i}\right) - \frac{\partial L}{\partial q_i} \tag{4}$$

$$L(\boldsymbol{q}, \dot{\boldsymbol{q}}) = E_{c_{Trans}} + E_{c_{Rot}} - E_p \tag{5}$$

where L is the Lagrangian of the helicopter model, $E_{c_{Trans}}$ is the translational kinetic energy, $E_{c_{Rot}}$ is the rotational kinetic energy, E_p is the total potential energy, $\boldsymbol{q} = [\boldsymbol{\xi}' \quad \boldsymbol{\eta}']' \in \Re^6$ is the generalized coordinates vector, $\boldsymbol{\tau}_{\eta} \in \Re^3$ represents the roll, pitch and yaw moments, and $\boldsymbol{f}_{\xi} = \boldsymbol{R}_{\mathscr{I}}\widehat{\boldsymbol{f}} + \boldsymbol{\alpha}_{\boldsymbol{T}}$ is the translational force applied to the helicopter due to the main control input U_1 in z axis direction, with $\boldsymbol{R}_{\mathscr{I}}\widehat{\boldsymbol{f}} = \boldsymbol{R}_{\mathscr{I}_{\boldsymbol{e_3}}}U_1$,[2] and $\boldsymbol{\alpha}_{\boldsymbol{T}} = [A_x \quad A_y \quad A_z]'$ are the aerodynamic forces vector, whose components are in the E_x, E_y and E_z axes, respectively. The aerodynamic forces are considered like external disturbances for the control design purposes.

Since the Lagrangian does not contain kinetic energy terms combining $\dot{\boldsymbol{\xi}}$ and $\dot{\boldsymbol{\eta}}$, the Lagrange–Euler equations can be divided into translational and rotational dynamics (see Fig. 2 — *Quadrotor Helicopter* block). The translational movement can be expressed by the following equation (Castillo, Lozano, & Dzul, 2005a; Raffo et al., 2008):

$$m\ddot{\boldsymbol{\xi}} + mg\boldsymbol{e_3} = \boldsymbol{f}_{\xi}. \tag{6}$$

Eq. (6) can be expressed by means of state vector $\boldsymbol{\xi}$, yielding:

$$\begin{cases} \ddot{x} = \dfrac{1}{m}\left(\cos\psi\sin\theta\cos\phi + \sin\psi\sin\phi\right)U_1 + \dfrac{A_x}{m} \\ \ddot{y} = \dfrac{1}{m}\left(\sin\psi\sin\theta\cos\phi - \cos\psi\sin\phi\right)U_1 + \dfrac{A_y}{m} \\ \ddot{z} = -g + \dfrac{1}{m}\left(\cos\theta\cos\phi\right)U_1 + \dfrac{A_z}{m} \end{cases} \tag{7}$$

where m is the helicopter mass and g is the gravitational acceleration.

The rotational kinetic energy equation must be rewritten to represent the equations of the rotational motion as a function of the generalized coordinate $\boldsymbol{\eta}$. Let $\boldsymbol{W}_{\eta}$ name the Jacobian from $\boldsymbol{\omega}$ to $\dot{\boldsymbol{\eta}}$ in (3), the following matrix is defined:

$$\mathscr{J} = \mathscr{J}(\boldsymbol{\eta}) = \boldsymbol{W}_{\eta}'\boldsymbol{J}\boldsymbol{W}_{\eta} \tag{8}$$

where $\boldsymbol{J}$ is the diagonal moment of inertia tensor. Then the rotational kinetic energy equation can be expressed as follows:

$$E_{c_{Rot}} = \frac{1}{2}\dot{\boldsymbol{\eta}}'\mathscr{J}\dot{\boldsymbol{\eta}}. \tag{9}$$

[1] The notation prime $'$ denotes transpose.

[2] The notation $\boldsymbol{e_3}$ represents the vector $\boldsymbol{e_3} = [0 \quad 0 \quad 1]'$. Thus, the therm $\boldsymbol{R}_{\mathscr{I}_{\boldsymbol{e_3}}}$ denotes the third column of the rotation matrix.

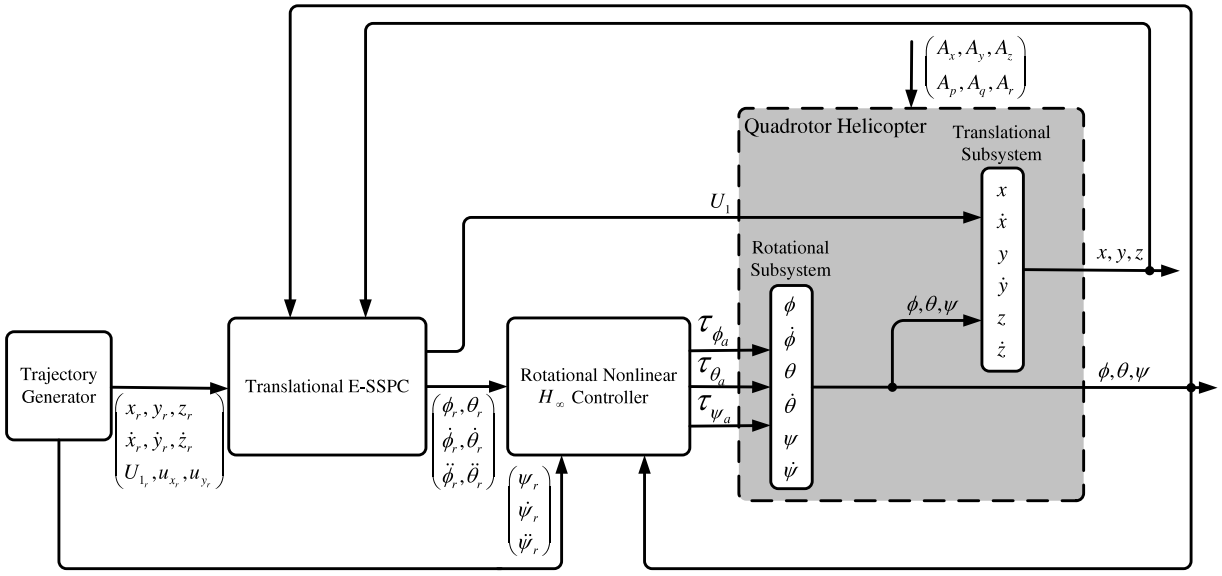

Fig. 2. Quadrotor helicopter control structure.

From the above expression, the Lagrange–Euler rotational equations in terms of $\boldsymbol{\eta}$ can be written, in general form, as follows (Castillo et al., 2005a):

$$\boldsymbol{M}(\boldsymbol{\eta})\ddot{\boldsymbol{\eta}} + \boldsymbol{C}(\boldsymbol{\eta}, \dot{\boldsymbol{\eta}})\dot{\boldsymbol{\eta}} = \boldsymbol{\tau}_{\boldsymbol{\eta}} \tag{10}$$

where $\boldsymbol{M}(\boldsymbol{\eta}) = \mathcal{J}(\boldsymbol{\eta})$, that is:

$$\boldsymbol{M}(\boldsymbol{\eta}) = \begin{bmatrix} I_{xx} & 0 & -I_{xx}S\theta \\ 0 & I_{yy}C^2\phi + I_{zz}S^2\phi & \left(I_{yy} - I_{zz}\right)C\phi S\phi C\theta \\ -I_{xx}S\theta & \left(I_{yy} - I_{zz}\right)C\phi S\phi C\theta & I_{xx}S^2\theta + I_{yy}S^2\phi C^2\theta + I_{zz}C^2\phi C^2\theta \end{bmatrix} \tag{11}$$

and

$$\boldsymbol{C}(\boldsymbol{\eta}, \dot{\boldsymbol{\eta}}) = \begin{bmatrix} c_{11} & c_{12} & c_{13} \\ c_{21} & c_{22} & c_{23} \\ c_{31} & c_{32} & c_{33} \end{bmatrix}$$

where

$$\begin{aligned}
c_{11} &= 0 \\
c_{12} &= \left(I_{yy} - I_{zz}\right)\left(\dot{\theta}C\phi S\phi + \dot{\psi}S^2\phi C\theta\right) + \left(I_{zz} - I_{yy}\right)\dot{\psi}C^2\phi C\theta \\
&\quad - I_{xx}\dot{\psi}C\theta \\
c_{13} &= \left(I_{zz} - I_{yy}\right)\dot{\psi}C\phi S\phi C^2\theta \\
c_{21} &= \left(I_{zz} - I_{yy}\right)\left(\dot{\theta}C\phi S\phi + \dot{\psi}S^2\phi C\theta\right) + \left(I_{yy} - I_{zz}\right)\dot{\psi}C^2\phi C\theta \\
&\quad + I_{xx}\dot{\psi}C\theta \\
c_{22} &= \left(I_{zz} - I_{yy}\right)\dot{\phi}C\phi S\phi \\
c_{23} &= -I_{xx}\dot{\psi}S\theta C\theta + I_{yy}\dot{\psi}S^2\phi C\theta S\theta + I_{zz}\dot{\psi}C^2\phi S\theta C\theta \\
c_{31} &= \left(I_{yy} - I_{zz}\right)\dot{\psi}C^2\theta S\phi C\phi - I_{xx}\dot{\theta}C\theta \\
c_{32} &= \left(I_{zz} - I_{yy}\right)\left(\dot{\theta}C\phi S\phi S\theta + \dot{\phi}S^2\phi C\theta\right) + \left(I_{yy} - I_{zz}\right)\dot{\phi}C^2\phi C\theta \\
&\quad + I_{xx}\dot{\psi}S\theta C\theta - I_{yy}\dot{\psi}S^2\phi S\theta C\theta - I_{zz}\dot{\psi}C^2\phi S\theta C\theta \\
c_{33} &= \left(I_{yy} - I_{zz}\right)\dot{\phi}C\phi S\phi C^2\theta - I_{yy}\dot{\theta}S^2\phi C\theta S\theta - I_{zz}\dot{\theta}C^2\phi C\theta S\theta \\
&\quad + I_{xx}\dot{\theta}C\theta S\theta.
\end{aligned}$$

Therefore, the mathematical model (used for the controller synthesis) that describes the helicopter rotational movement obtained from the Lagrange–Euler formalism is given by:

$$\ddot{\boldsymbol{\eta}} = \boldsymbol{M}(\boldsymbol{\eta})^{-1}\left(\boldsymbol{\tau}_{\boldsymbol{\eta}} - \boldsymbol{C}(\boldsymbol{\eta}, \dot{\boldsymbol{\eta}})\dot{\boldsymbol{\eta}}\right). \tag{12}$$

3. Control strategy

To achieve a robust path following for the quadrotor helicopter, two techniques, capable of controlling the helicopter in presence of sustained external disturbances, parametric uncertainties and unmodelled dynamics, are combined. The proposed control strategy is based on the decentralized structure of the quadrotor helicopter system (4), which is composed of the dynamic Eqs. (6) and (10). The overall scheme of the control strategy is depicted in Fig. 2.

Firstly, the reference trajectory for the translational movements is provided off-line by the *Trajectory Generator* block. The computation of this trajectory is based on a virtual reference vehicle whose model is the same as the one of the quadrotor helicopter for the translational motion. Thereby, starting from a desired route for the translational movements, x_r, y_r, and z_r, and their derivatives, the reference control inputs U_{1_r}, u_{x_r} and u_{y_r}, are computed. The yaw reference angle is defined separately. This trajectory is generated under the following assumptions: there are no external disturbances acting on the virtual vehicle; and the attitude of the virtual vehicle is supposed to be stabilized.

A predictive controller is proposed to control the quadrotor translational movements in an outer loop, using the references provided by the trajectory generator. The state-space predictive controller based on the error model (E-SSPC) also includes the integral of the position error in the state vector in order to achieve null steady-state error when sustained disturbances are considered.

The translational motion control is performed in two stages. In the first one, the helicopter height, z, is controlled and the total thrust, U_1, is the manipulated signal. In the second stage, the reference of pitch and roll angles (θ_r and ϕ_r, respectively) are generated through the two virtual inputs, computed to follow the desired xy movement. In this second step, the control variable U_1 is used as a time-varying parameter.

Finally, a nonlinear $\mathcal{H}_\infty$ controller for the rotational subsystem is used in an inner loop to perform the quadrotor helicopter stabilization. The angular position and velocity are controlled in this loop, being the torques applied on the three axis, $\boldsymbol{\tau}_{\boldsymbol{\eta}_a} = [\tau_{\phi_a}\ \tau_{\theta_a}\ \tau_{\psi_a}]'$ (see Eq. (19)), the manipulated variables. To obtain null steady-state error in presence of sustained external disturbances, the integral of the angular position error is also considered. Due to the cascade structure of this strategy and taking into

account the closed-loop performance achieved by the inner nonlinear $\mathcal{H}_\infty$ controller loop, the Euler angles can be considered as time-varying parameters on the design of the translational controller.

The development of these controllers is analyzed in the following sections.

4. Nonlinear $\mathcal{H}_\infty$ controller for stabilization

In this section, a nonlinear $\mathcal{H}_\infty$ controller for the rotational subsystem is developed to achieve robustness in the presence of sustained disturbances, and parametric and structural uncertainties.

4.1. Nonlinear $\mathcal{H}_\infty$ control approach

The dynamic equation of a nth order smooth nonlinear system which is affected by an unknown disturbance can be expressed as follows:

$$\dot{\boldsymbol{x}} = f(\boldsymbol{x}, t) + g(\boldsymbol{x}, t)\boldsymbol{u} + k(\boldsymbol{x}, t)\boldsymbol{d}, \tag{13}$$

where $\boldsymbol{u} \in \Re^p$ is the vector of control inputs, $\boldsymbol{d} \in \Re^q$ is the vector of external disturbances and $\boldsymbol{x} \in \Re^n$ is the vector of states. Performance can be defined using the cost variable $\boldsymbol{\zeta} \in \Re^{(m+p)}$ given by the expression:

$$\boldsymbol{\zeta} = \boldsymbol{W}\begin{bmatrix} h(\boldsymbol{x}) \\ \boldsymbol{u} \end{bmatrix}, \tag{14}$$

where $h(\boldsymbol{x}) \in \Re^m$ represents a function of the vector of states to be controlled and $\boldsymbol{W} \in \Re^{(m+p)\times(m+p)}$ is a weighting matrix. If the states $\boldsymbol{x}$ are assumed to be available for measurement, then the optimal $\mathcal{H}_\infty$ problem can be posed as follows (Van der Schaft, 1992):

Find the smallest value $\gamma^* \geq 0$ such that for any $\gamma \geq \gamma^*$ there exists a state feedback $\boldsymbol{u} = \boldsymbol{u}(\boldsymbol{x}, t)$, such that the L_2 gain from $\boldsymbol{d}$ to $\boldsymbol{\zeta}$ is less than or equal to γ, that is:

$$\int_0^T \|\boldsymbol{\zeta}\|_2^2 \,\mathrm{d}t \leq \gamma^2 \int_0^T \|\boldsymbol{d}\|_2^2 \,\mathrm{d}t. \tag{15}$$

The internal term of the integral expression on the left-hand side of inequality (15) can be written as:

$$\|\boldsymbol{\zeta}\|_2^2 = \boldsymbol{\zeta}'\boldsymbol{\zeta} = \begin{bmatrix} h'(\boldsymbol{x}) & \boldsymbol{u}' \end{bmatrix} \boldsymbol{W}'\boldsymbol{W} \begin{bmatrix} h(\boldsymbol{x}) \\ \boldsymbol{u} \end{bmatrix}$$

and the symmetric positive definite matrix $\boldsymbol{W}'\boldsymbol{W}$ can be partitioned as follows:

$$\boldsymbol{W}'\boldsymbol{W} = \begin{bmatrix} \boldsymbol{Q} & \boldsymbol{S} \\ \boldsymbol{S}' & \boldsymbol{R} \end{bmatrix}. \tag{16}$$

Matrices $\boldsymbol{Q}$ and $\boldsymbol{R}$ are symmetric positive definite and the fact that $\boldsymbol{W}'\boldsymbol{W} > \boldsymbol{O}$ guarantees that $\boldsymbol{Q} - \boldsymbol{S}\boldsymbol{R}^{-1}\boldsymbol{S}' > \boldsymbol{O}$, where $\boldsymbol{O}$ is the nth order zero matrix.

Under these assumptions, an optimal control signal $\boldsymbol{u}^*(\boldsymbol{x}, t)$ may be computed for system (13) if there is a smooth solution $V(\boldsymbol{x}, t)$, with $V(\boldsymbol{x}_0, t) \equiv 0$ for $t \geq 0$, to the following HJBI equation (Van der Schaft, 2000):

$$\begin{aligned} &\frac{\partial V}{\partial t} + \frac{\partial' V}{\partial \boldsymbol{x}} f(\boldsymbol{x}, t) \\ &\quad + \frac{1}{2}\frac{\partial' V}{\partial \boldsymbol{x}}\left[\frac{1}{\gamma^2}k(\boldsymbol{x}, t)k'(\boldsymbol{x}, t) - g(\boldsymbol{x}, t)\boldsymbol{R}^{-1}g'(\boldsymbol{x}, t)\right]\frac{\partial V}{\partial \boldsymbol{x}} \\ &\quad - \frac{\partial' V}{\partial \boldsymbol{x}} g(\boldsymbol{x}, t)\boldsymbol{R}^{-1}\boldsymbol{S}'h(\boldsymbol{x}) + \frac{1}{2}h'(\boldsymbol{x})\left(\boldsymbol{Q} - \boldsymbol{S}\boldsymbol{R}^{-1}\boldsymbol{S}'\right)h(\boldsymbol{x}) = 0 \end{aligned} \tag{17}$$

for each $\gamma > \sqrt{\sigma_{\max}(\boldsymbol{R})} \geq 0$, where $\sigma_{\max}$ stands for the maximum singular value. In such a case, the optimal state feedback control law is derived as follows (Feng & Postlethwaite, 1994):

$$\boldsymbol{u}^* = -\boldsymbol{R}^{-1}\left(\boldsymbol{S}'h(\boldsymbol{x}) + g'(\boldsymbol{x}, t)\frac{\partial V(\boldsymbol{x}, t)}{\partial \boldsymbol{x}}\right). \tag{18}$$

4.2. Rotational subsystem nonlinear $\mathcal{H}_\infty$ control

The rotational movements dynamic model (10), obtained from the Lagrange–Euler formalism, is used in order to develop the nonlinear $\mathcal{H}_\infty$ controller. $\boldsymbol{\tau}_\eta$ joins the control torques and external disturbances, and is redefined as:

$$\boldsymbol{\tau}_\eta = \boldsymbol{\tau}_{\eta_a} + \boldsymbol{\tau}_{\eta_d} \tag{19}$$

where $\boldsymbol{\tau}_{\eta_a}$ is the applied torques vector and $\boldsymbol{\tau}_{\eta_d}$ represents the total effect of system modelling errors and external disturbances.

As a first step to synthesize the control law, the tracking error vector is defined as follows:

$$\boldsymbol{x}_\eta = \begin{bmatrix} \dot{\tilde{\boldsymbol{\eta}}} \\ \tilde{\boldsymbol{\eta}} \\ \int \tilde{\boldsymbol{\eta}}\mathrm{d}t \end{bmatrix} = \begin{bmatrix} \dot{\boldsymbol{\eta}} - \dot{\boldsymbol{\eta}}_{\boldsymbol{r}} \\ \boldsymbol{\eta} - \boldsymbol{\eta}_{\boldsymbol{r}} \\ \int \left(\boldsymbol{\eta} - \boldsymbol{\eta}_{\boldsymbol{r}}\right)\mathrm{d}t \end{bmatrix} \tag{20}$$

where $\boldsymbol{\eta}_{\boldsymbol{r}}$ and $\dot{\boldsymbol{\eta}}_{\boldsymbol{r}} \in \Re^n$ are the desired trajectory and the corresponding velocity, respectively. Note that an integral term has been included in the error vector. This term will allow the achievement of a null steady-state error when persistent disturbances are acting on the system (Ortega et al., 2005).

The following control law is proposed for the rotational subsystem (Ortega et al., 2005):

$$\begin{aligned} \boldsymbol{\tau}_{\eta_a} &= \boldsymbol{M}(\boldsymbol{\eta})\ddot{\boldsymbol{\eta}} + \boldsymbol{C}(\boldsymbol{\eta}, \dot{\boldsymbol{\eta}})\dot{\boldsymbol{\eta}} \\ &\quad - \boldsymbol{T}_1^{-1}\left(\boldsymbol{M}(\boldsymbol{\eta})\boldsymbol{T}\dot{\boldsymbol{x}}_\eta + \boldsymbol{C}(\boldsymbol{\eta}, \dot{\boldsymbol{\eta}})\boldsymbol{T}\boldsymbol{x}_\eta\right) + \boldsymbol{T}_1^{-1}\boldsymbol{u}. \end{aligned} \tag{21}$$

The proposed control law can be split up into three different parts: the first one consists of the first two terms of that equation, which are designed in order to compensate the system dynamics (10). The second part consists of two terms including the error vector $\boldsymbol{x}_\eta$ and its derivative, $\dot{\boldsymbol{x}}_\eta$. Assuming $\boldsymbol{\tau}_{\eta_d} \equiv \boldsymbol{0}$, these two terms of the control law enable perfect tracking, which means that they represent the *essential* control effort needed to perform the task. Finally, the third part includes a vector $\boldsymbol{u}$, which represents the *additional* control effort needed for disturbance rejection.

It can also be pointed out that, despite it seeming that the preceding control law might not seem a well posed system, it will be shown afterwards that the computed torque does not rely on joint accelerations, but on their references.

Matrix $\boldsymbol{T}$ in (21) can be partitioned as follows:

$$\boldsymbol{T} = \begin{bmatrix} \boldsymbol{T}_1 & \boldsymbol{T}_2 & \boldsymbol{T}_3 \end{bmatrix}$$

with $\boldsymbol{T}_1 = \rho\boldsymbol{I}$, where ρ is a positive scalar and $\boldsymbol{I}$ is the nth order identity matrix.

Substituting the expression of the control law from (21) into the Lagrange–Euler equation of the system (10) and defining $\boldsymbol{d} = \boldsymbol{M}(\boldsymbol{\eta})\boldsymbol{T}_1\boldsymbol{M}^{-1}(\boldsymbol{\eta})\boldsymbol{\tau}_{\eta_d}$, the following expression is obtained:

$$\boldsymbol{M}(\boldsymbol{\eta})\boldsymbol{T}\dot{\boldsymbol{x}}_\eta + \boldsymbol{C}(\boldsymbol{\eta}, \dot{\boldsymbol{\eta}})\boldsymbol{T}\boldsymbol{x}_\eta = \boldsymbol{u} + \boldsymbol{d}. \tag{22}$$

The above expression represents the *dynamic equation of the system error*. Taking into account this nonlinear equation, the nonlinear $\mathcal{H}_\infty$ control problem can be posed as follows:

"Find a control law $\boldsymbol{u}(t)$ such that the ratio between the energy of the cost variable $\boldsymbol{\zeta} = \boldsymbol{W}\left[h'(\boldsymbol{x}_\eta)\boldsymbol{u}'\right]'$ and the energy of the disturbance signals $\boldsymbol{d}$ is less than a given attenuation level γ".

Taking into account the definition of the vector error, $\boldsymbol{x}_\eta$, and the definition of the cost variable, $\boldsymbol{\zeta}$, the following structures are considered for matrices $\boldsymbol{Q}$ and $\boldsymbol{S}$ in (16):

$$\boldsymbol{Q} = \begin{bmatrix} \boldsymbol{Q}_1 & \boldsymbol{Q}_{12} & \boldsymbol{Q}_{13} \\ \boldsymbol{Q}_{12} & \boldsymbol{Q}_2 & \boldsymbol{Q}_{23} \\ \boldsymbol{Q}_{13} & \boldsymbol{Q}_{23} & \boldsymbol{Q}_3 \end{bmatrix}, \qquad \boldsymbol{S} = \begin{bmatrix} \boldsymbol{S}_1 \\ \boldsymbol{S}_2 \\ \boldsymbol{S}_3 \end{bmatrix}.$$

To apply the theoretical results presented in Section 4.1, it is necessary to rewrite the nonlinear dynamic equation of the error

(22) into the standard form of the nonlinear $\mathcal{H}_\infty$ problem (see (13)). This can be done by defining the following expressions:

$$\dot{\boldsymbol{x}}_\eta = f(\boldsymbol{x}_\eta, t) + g(\boldsymbol{x}_\eta, t)\boldsymbol{u} + k(\boldsymbol{x}_\eta, t)\boldsymbol{d}, \tag{23}$$

$$f\left(\boldsymbol{x}_\eta, t\right) = \boldsymbol{T}_0^{-1}\begin{bmatrix} -\boldsymbol{M}(\boldsymbol{\eta})^{-1}\boldsymbol{C}(\boldsymbol{\eta}, \dot{\boldsymbol{\eta}}) & \boldsymbol{O} & \boldsymbol{O} \\ \boldsymbol{T}_1^{-1} & \boldsymbol{I} - \boldsymbol{T}_1^{-1}\boldsymbol{T}_2 & -\boldsymbol{I} + \boldsymbol{T}_1^{-1}(\boldsymbol{T}_2 - \boldsymbol{T}_3) \\ \boldsymbol{O} & \boldsymbol{I} & -\boldsymbol{I} \end{bmatrix}\boldsymbol{T}_0\boldsymbol{x}_\eta,$$

$$g\left(\boldsymbol{x}_\eta, t\right) = k\left(\boldsymbol{x}_\eta, t\right) = \boldsymbol{T}_0^{-1}\begin{bmatrix} \boldsymbol{M}(\boldsymbol{\eta})^{-1} \\ \boldsymbol{O} \\ \boldsymbol{O} \end{bmatrix}$$

where

$$\boldsymbol{T}_0 = \begin{bmatrix} \boldsymbol{T}_1 & \boldsymbol{T}_2 & \boldsymbol{T}_3 \\ \boldsymbol{O} & \boldsymbol{I} & \boldsymbol{I} \\ \boldsymbol{O} & \boldsymbol{O} & \boldsymbol{I} \end{bmatrix}. \tag{24}$$

As stated in Section 4.1, the solution of the HJBI equation depends on the choice of the cost variable, $\boldsymbol{\zeta}$, and particularly on the selection of function $h(\boldsymbol{x}_\eta)$ (see (14)). In this paper, this function is taken to be equal to the error vector. That is, $h(\boldsymbol{x}_\eta) = \boldsymbol{x}_\eta$. Once this function has been selected, computing the control law $\boldsymbol{u}$ will require finding the Lyapunov function, $V(\boldsymbol{x}_\eta, t)$, to the HJBI equation posed in the previous section (see (17)).

The following theorem will help do this.

Theorem. *Let $V(\boldsymbol{x}_\eta, t)$ be the scalar function:*

$$V\left(\boldsymbol{x}_\eta, t\right) = \frac{1}{2}\boldsymbol{x}_\eta'\boldsymbol{T}_0'\begin{bmatrix} \boldsymbol{M}(\boldsymbol{\eta}) & \boldsymbol{O} & \boldsymbol{O} \\ \boldsymbol{O} & \boldsymbol{Y} & \boldsymbol{X} - \boldsymbol{Y} \\ \boldsymbol{O} & \boldsymbol{X} - \boldsymbol{Y} & \boldsymbol{Z} + \boldsymbol{Y} \end{bmatrix}\boldsymbol{T}_0\boldsymbol{x}_\eta, \tag{25}$$

where $\boldsymbol{X}$, $\boldsymbol{Y}$ and $\boldsymbol{Z} \in \Re^{n\times n}$ are constant, symmetric, and positive definite matrices such that $\boldsymbol{Z} - \boldsymbol{X}\boldsymbol{Y}^{-1}\boldsymbol{X} + 2\boldsymbol{X} > \boldsymbol{O}$, and $\boldsymbol{T}_0$ is as defined in (24). Let $\boldsymbol{T}$ be the matrix appearing in (22). If these matrices verify the following equation:

$$\begin{bmatrix} \boldsymbol{O} & \boldsymbol{Y} & \boldsymbol{X} \\ \boldsymbol{Y} & 2\boldsymbol{X} & \boldsymbol{Z} + 2\boldsymbol{X} \\ \boldsymbol{X} & \boldsymbol{Z} + 2\boldsymbol{X} & \boldsymbol{O} \end{bmatrix} + \boldsymbol{Q} + \frac{1}{\gamma^2}\boldsymbol{T}'\boldsymbol{T} - \left(\boldsymbol{S}' + \boldsymbol{T}\right)'\boldsymbol{R}^{-1}\left(\boldsymbol{S}' + \boldsymbol{T}\right) = \boldsymbol{O} \tag{26}$$

then, function $V(\boldsymbol{x}_\eta, t)$ constitutes a solution to the HJBI, for a sufficiently high value of γ.

The proof of this theorem is obtained following the steps presented in Ortega et al. (2005). ◇

Once matrix $\boldsymbol{T} = \begin{bmatrix} \boldsymbol{T}_1 & \boldsymbol{T}_2 & \boldsymbol{T}_3 \end{bmatrix}$ is computed by solving some Riccati algebraic equations, substituting $V\left(\boldsymbol{x}_\eta, t\right)$ in (18), control law $\boldsymbol{u}^*$ corresponding to the $\mathcal{H}_\infty$ optimal index γ is given by

$$\boldsymbol{u}^* = -\boldsymbol{R}^{-1}\left(\boldsymbol{S}' + \boldsymbol{T}\right)\boldsymbol{x}_\eta. \tag{27}$$

Finally, if the control law (27) is replaced into (21), and after some manipulations, the optimal control law can be written as:

$$\boldsymbol{\tau}_{\eta a}^* = \boldsymbol{M}(\boldsymbol{\eta})\ddot{\boldsymbol{\eta}}_{\boldsymbol{r}} + \boldsymbol{C}(\boldsymbol{\eta}, \dot{\boldsymbol{\eta}})\dot{\boldsymbol{\eta}} - \boldsymbol{M}(\boldsymbol{\eta})\left(\boldsymbol{K}_{\boldsymbol{D}}\dot{\tilde{\boldsymbol{\eta}}} + \boldsymbol{K}_{\boldsymbol{P}}\tilde{\boldsymbol{\eta}} - \boldsymbol{K}_{\boldsymbol{I}}\int\tilde{\boldsymbol{\eta}}\mathrm{d}t\right) \tag{28}$$

where

$$\boldsymbol{K}_{\boldsymbol{D}} = \boldsymbol{T}_1^{-1}\left(\boldsymbol{T}_2 + \boldsymbol{M}(\boldsymbol{\eta})^{-1}\boldsymbol{C}(\boldsymbol{\eta}, \dot{\boldsymbol{\eta}})\boldsymbol{T}_1 + \boldsymbol{M}(\boldsymbol{\eta})^{-1}\boldsymbol{R}^{-1}\left(\boldsymbol{S}_1' + \boldsymbol{T}_1\right)\right)$$
$$\boldsymbol{K}_{\boldsymbol{P}} = \boldsymbol{T}_1^{-1}\left(\boldsymbol{T}_3 + \boldsymbol{M}(\boldsymbol{\eta})^{-1}\boldsymbol{C}(\boldsymbol{\eta}, \dot{\boldsymbol{\eta}})\boldsymbol{T}_2 + \boldsymbol{M}(\boldsymbol{\eta})^{-1}\boldsymbol{R}^{-1}\left(\boldsymbol{S}_2' + \boldsymbol{T}_2\right)\right)$$
$$\boldsymbol{K}_{\boldsymbol{I}} = -\boldsymbol{T}_1^{-1}\left(\boldsymbol{M}(\boldsymbol{\eta})^{-1}\boldsymbol{C}(\boldsymbol{\eta}, \dot{\boldsymbol{\eta}})\boldsymbol{T}_3 + \boldsymbol{M}(\boldsymbol{\eta})^{-1}\boldsymbol{R}^{-1}\left(\boldsymbol{S}_3' + \boldsymbol{T}_3\right)\right).$$

A particular case can be obtained when the components of weighting compound $\boldsymbol{W}'\boldsymbol{W}$ verify:

$$\boldsymbol{Q}_1 = {\omega_1}^2\boldsymbol{I}, \quad \boldsymbol{Q}_2 = {\omega_2}^2\boldsymbol{I}, \quad \boldsymbol{Q}_3 = {\omega_3}^2\boldsymbol{I}, \quad \boldsymbol{R} = {\omega_u}^2\boldsymbol{I}, \tag{29}$$

$$\boldsymbol{Q}_{12} = \boldsymbol{Q}_{13} = \boldsymbol{Q}_{23} = \boldsymbol{O}, \quad \boldsymbol{S}_1 = \boldsymbol{S}_2 = \boldsymbol{S}_3 = \boldsymbol{O}.$$

In this case, the following analytical expressions for the gain matrices have been obtained:

$$\boldsymbol{K}_{\boldsymbol{D}} = \frac{\sqrt{{\omega_2}^2 + 2\omega_1\omega_3}}{\omega_1}\boldsymbol{I} + \boldsymbol{M}(\boldsymbol{\eta})^{-1}\left(\boldsymbol{C}(\boldsymbol{\eta}, \dot{\boldsymbol{\eta}}) + \frac{1}{{\omega_u}^2}\boldsymbol{I}\right),$$
$$\boldsymbol{K}_{\boldsymbol{P}} = \frac{\omega_3}{\omega_1}\boldsymbol{I} + \frac{\sqrt{{\omega_2}^2 + 2\omega_1\omega_3}}{\omega_1}\boldsymbol{M}(\boldsymbol{\eta})^{-1}\left(\boldsymbol{C}(\boldsymbol{\eta}, \dot{\boldsymbol{\eta}}) + \frac{1}{{\omega_u}^2}\boldsymbol{I}\right),$$
$$\boldsymbol{K}_{\boldsymbol{I}} = \frac{\omega_3}{\omega_1}\boldsymbol{M}(\boldsymbol{\eta})^{-1}\left(\boldsymbol{C}(\boldsymbol{\eta}, \dot{\boldsymbol{\eta}}) + \frac{1}{{\omega_u}^2}\boldsymbol{I}\right)$$

where the parameters ω_1, ω_2, ω_3 and ω_u can be tuned by a systematic procedure keeping in mind a linear PID control action interpretation.

These expressions have an important property: they do not depend on the parameter γ. So, we obtain an algebraic expression for computing the general optimal solution for this particular case.

5. E-SSPC for path following

In this section a control law to solve the path following problem by translational movements is designed. A linear state-space MPC strategy based on the error model (E-SSPC) is performed. From the error model, two predictive controllers are synthesized. The first one controls the height through the input U_1, whereas the second one makes use of this signal as a time variant parameter in the linear x and y motions to compute two virtual inputs, $\bar{u}_x$ and $\bar{u}_y$.

The system (7) can be rewritten in a state-space form as $\dot{\bar{\boldsymbol{\xi}}}(t) = f\left(\bar{\boldsymbol{\xi}}(t), \boldsymbol{u}_{\bar{\boldsymbol{\xi}}}(t)\right)$ for the controller design, where $\bar{\boldsymbol{\xi}}(t) = [x(t) \quad u_0(t) \quad y(t) \quad v_0(t) \quad z(t) \quad w_0(t)]'$ stands for the state-space vector of the system, where $u_0(t)$, $v_0(t)$, and $w_0(t)$ are the components of the linear velocity of the vehicle mass center expressed in the inertial frame (see Eq. (2)).

From (7) and the new state-space vector, the system dynamic equation to control design can be written in the following form:

$$\dot{\bar{\boldsymbol{\xi}}}(t) = f\left(\bar{\boldsymbol{\xi}}(t), \boldsymbol{u}_{\bar{\boldsymbol{\xi}}}(t)\right) = \begin{bmatrix} u_0(t) \\ u_x(t)\dfrac{U_1(t)}{m} + \dfrac{A_x(t)}{m} \\ v_0(t) \\ u_y(t)\dfrac{U_1(t)}{m} + \dfrac{A_y(t)}{m} \\ w_0(t) \\ -g + (\cos\theta(t)\cos\phi(t))\dfrac{U_1(t)}{m} + \dfrac{A_z(t)}{m} \end{bmatrix} \tag{30}$$

with:

$$u_x(t) \triangleq \cos\psi(t)\sin\theta(t)\cos\phi(t) + \sin\psi(t)\sin\phi(t)$$
$$u_y(t) \triangleq \sin\psi(t)\sin\theta(t)\cos\phi(t) - \cos\psi(t)\sin\phi(t). \tag{31}$$

Eqs. (7) show that the movement through the x and y axes depends on the control input U_1. In fact, U_1 is the designed total thrust magnitude to obtain the desired linear movement, while u_x and u_y can be considered as the directions of U_1 that cause the movement through the x and y axes, respectively.

The objective of this approach is to guarantee that the UAV follows a previously defined reference trajectory minimizing the displacement error. However, due to the fact that the target coordinates vary in time, a virtual reference vehicle with the same quadrotor helicopter mathematical model is defined:

$$\dot{\bar{\boldsymbol{\xi}}}_{\boldsymbol{r}}(t) = f\left(\bar{\boldsymbol{\xi}}_{\boldsymbol{r}}(t), \boldsymbol{u}_{\boldsymbol{\xi r}}(t)\right) \tag{32}$$

where $\bar{\boldsymbol{\xi}}_{\boldsymbol{r}}(t) = [x_r(t) \quad u_{0_r}(t) \quad y_r(t) \quad v_{0_r}(t) \quad z_r(t) \quad w_{0_r}(t)]'$ and $\boldsymbol{u}_{\boldsymbol{\xi r}}(t) = [u_{x_r} \quad u_{y_r} \quad U_{1_r}]'$ are the reference states and the control inputs, respectively. Null external disturbances are assumed in the virtual reference vehicle. This virtual reference vehicle is used to obtain the reference control inputs for translational movements under the assumption that the helicopter height has been stabilized. Therefore, for the case of this vehicle, the reference values are given by:

$$U_{1_r} = m \cdot (\ddot{z}_r + g), \qquad u_{x_r} = \frac{\ddot{x}_r \cdot m}{U_{1_r}}, \qquad u_{y_r} = \frac{\ddot{y}_r \cdot m}{U_{1_r}}.$$

By subtracting the virtual reference vehicle (32) from the system (30), the proposed translational error model is given by:

$$\dot{\tilde{\boldsymbol{\xi}}}(t) = \boldsymbol{A}(t) \cdot \tilde{\boldsymbol{\xi}}(t) + \boldsymbol{B}(t) \cdot \tilde{\boldsymbol{u}}_{\boldsymbol{\xi}}(t) \tag{33}$$

where $\tilde{\boldsymbol{\xi}}(t) = \bar{\boldsymbol{\xi}}(t) - \bar{\boldsymbol{\xi}}_{\boldsymbol{r}}(t)$ represents the error vector, and $\tilde{\boldsymbol{u}}_{\boldsymbol{\xi}}(t) = \boldsymbol{u}_{\boldsymbol{\xi}}(t) - \boldsymbol{u}_{\boldsymbol{\xi r}}(t)$ is the control input error. Matrices $\boldsymbol{A}(t)$ and $\boldsymbol{B}(t)$ are the Jacobians of the system (30) in relation to $\bar{\boldsymbol{\xi}}(t)$ and $\boldsymbol{u}_{\boldsymbol{\xi}}(t)$, respectively. Besides, the integral of the position error term has been included in the error vector to perform an appropriate path following in presence of sustained disturbances. Therefore, the following augmented error vector is considered:

$$\boldsymbol{x}_{\boldsymbol{\xi}}(t) = \begin{bmatrix} \tilde{x}(t) \\ \tilde{u}_0(t) \\ \int \tilde{x}(t)\mathrm{d}t \\ \tilde{y}(t) \\ \tilde{v}_0(t) \\ \int \tilde{y}(t)\mathrm{d}t \\ \tilde{z}(t) \\ \tilde{w}_0(t) \\ \int \tilde{z}(t)\mathrm{d}t \end{bmatrix} = \begin{bmatrix} x(t) - x_r(t) \\ u_0(t) - u_{0_r}(t) \\ \int (x(t) - x_r(t))\mathrm{d}t \\ y(t) - y_r(t) \\ v_0(t) - v_{0_r}(t) \\ \int (y(t) - y_r(t))\mathrm{d}t \\ z(t) - z_r(t) \\ w_0(t) - w_{0_r}(t) \\ \int (z(t) - z_r(t))\mathrm{d}t \end{bmatrix}. \tag{34}$$

Using Euler's method, a time-varying discrete linear model is obtained, i.e.:

$$\boldsymbol{x}_{\boldsymbol{\xi}}(k+1) = \overline{\boldsymbol{A}} \cdot \boldsymbol{x}_{\boldsymbol{\xi}}(k) + \overline{\boldsymbol{B}}(k) \cdot \tilde{\boldsymbol{u}}_{\boldsymbol{\xi}}(k). \tag{35}$$

The input control $U_1(t)$ is considered as a time-varying parameter for the reference x and y motions. Moreover, because of the decentralized control structure, the roll, pitch and yaw angles are also considered as time-varying parameters.

The error model (35) can be split up into two subsystems: the height error and the x and y motions error. Matrices $\overline{\boldsymbol{A}}$ and $\overline{\boldsymbol{B}}$ for each subsystem are the following:

$$\overline{\boldsymbol{A}}_z = \begin{bmatrix} 1 & \Delta t & 0 \\ 0 & 1 & 0 \\ \Delta t & 0 & 1 \end{bmatrix}, \qquad \overline{\boldsymbol{B}}_z = \begin{bmatrix} 0 \\ \dfrac{\Delta t}{m}\cos\theta(k)\cos\phi(k) \\ 0 \end{bmatrix} \tag{36}$$

$$\overline{\boldsymbol{A}}_{xy} = \begin{bmatrix} 1 & \Delta t & 0 & 0 & 0 & 0 \\ 0 & 1 & 0 & 0 & 0 & 0 \\ \Delta t & 0 & 1 & 0 & 0 & 0 \\ 0 & 0 & 0 & 1 & \Delta t & 0 \\ 0 & 0 & 0 & 0 & 1 & 0 \\ 0 & 0 & 0 & \Delta t & 0 & 1 \end{bmatrix},$$

$$\overline{\boldsymbol{B}}_{xy} = \begin{bmatrix} 0 & 0 \\ \dfrac{\Delta t}{m}U_1(k) & 0 \\ 0 & 0 \\ 0 & 0 \\ 0 & \dfrac{\Delta t}{m}U_1(k) \\ 0 & 0 \end{bmatrix} \tag{37}$$

where Δt is the sampling time, which has been chosen sufficiently small to capture all translational motion error dynamic and high enough to consider the rotational closed-loop dynamics in steady state.

Based on this analysis, the path following problem for a UAV can be understood as: find the control inputs in a bounded group of possible values that drive the state variables in (35) from an initial position $\boldsymbol{x}_{\boldsymbol{\xi}_0}$ to the origin (Sun, 2005), i.e. $\lim_{t\to\infty} \boldsymbol{x}_{\boldsymbol{\xi}} = 0$.

Therefore, from the height and longitudinal–lateral error models the control laws can be designed in such a way that the system is forced to track the reference trajectory. The first law computes the control input U_1 in such a way that the following cost is minimized:

$$J_z = \left[\widehat{\boldsymbol{x}}_{\boldsymbol{\xi}z} - \widehat{\boldsymbol{x}}_{\boldsymbol{\xi r}z}\right]' \boldsymbol{Q}_z \left[\widehat{\boldsymbol{x}}_{\boldsymbol{\xi}z} - \widehat{\boldsymbol{x}}_{\boldsymbol{\xi r}z}\right] + \left[\widehat{\widetilde{\boldsymbol{u}}}_{\boldsymbol{\xi}z} - \widehat{\widetilde{\boldsymbol{u}}}_{\boldsymbol{\xi r}z}\right]' \boldsymbol{R}_z \left[\widehat{\widetilde{\boldsymbol{u}}}_{\boldsymbol{\xi}z} - \widehat{\widetilde{\boldsymbol{u}}}_{\boldsymbol{\xi r}z}\right] + \Omega\left(\widehat{\boldsymbol{x}}_{\boldsymbol{\xi}z}(k + \boldsymbol{N}_{\boldsymbol{2}_z}|k) - \widehat{\boldsymbol{x}}_{\boldsymbol{\xi r}z}(k + \boldsymbol{N}_{\boldsymbol{2}_z}|k)\right) \tag{38}$$

where $\boldsymbol{Q}_z$ and $\boldsymbol{R}_z$ are diagonal definite positive weighting matrices, $\boldsymbol{N}_{\boldsymbol{2}_z}$ is the prediction horizon (Rossiter, 2003), and Ω is the terminal state cost defined by:

$$\begin{aligned}\Omega&\left(\widehat{\boldsymbol{x}}_{\boldsymbol{\xi}z}(k + \boldsymbol{N}_{\boldsymbol{2}_z}|k) - \widehat{\boldsymbol{x}}_{\boldsymbol{\xi r}z}(k + \boldsymbol{N}_{\boldsymbol{2}_z}|k)\right) \\ &= \left[\widehat{\boldsymbol{x}}_{\boldsymbol{\xi}z}(k + \boldsymbol{N}_{\boldsymbol{2}_z}|k) - \widehat{\boldsymbol{x}}_{\boldsymbol{\xi r}z}(k + \boldsymbol{N}_{\boldsymbol{2}_z}|k)\right]' \\ &\quad \times \boldsymbol{P}_z \left[\widehat{\boldsymbol{x}}_{\boldsymbol{\xi}z}(k + \boldsymbol{N}_{\boldsymbol{2}_z}|k) - \widehat{\boldsymbol{x}}_{\boldsymbol{\xi r}z}(k + \boldsymbol{N}_{\boldsymbol{2}_z}|k)\right]\end{aligned}$$

with $\boldsymbol{P}_z \geq 0$ (Kühne, Lages, & Gomes Da Silva, 2005).

The predictions of the model output $\widehat{\boldsymbol{x}}_{\boldsymbol{\xi}z}(k + j|k)$ are computed using a linearized time-varying state-space model of the vehicle by the Eqs. (35) and (36), obtaining:

$$\widehat{\boldsymbol{x}}_{\boldsymbol{\xi}z} = \boldsymbol{P}_z(k|k) \cdot \boldsymbol{x}_{\boldsymbol{\xi}z}(k|k) + \boldsymbol{H}_z(k|k) \cdot \widehat{\widetilde{\boldsymbol{u}}}_{\boldsymbol{\xi}z}, \tag{39}$$

where $\widetilde{\boldsymbol{u}}_{\boldsymbol{\xi}z}(k|k) = U_1(k) - U_{1_r}(k)$, and $\boldsymbol{x}_{\boldsymbol{\xi}z}(k)$ is the height state error vector. The height reference vectors are:

$$\widehat{\boldsymbol{x}}_{\boldsymbol{\xi r}z} \triangleq \begin{bmatrix} \boldsymbol{x}_{\boldsymbol{\xi r}z}(k+1|k) - \boldsymbol{x}_{\boldsymbol{\xi r}z}(k|k) \\ \vdots \\ \boldsymbol{x}_{\boldsymbol{\xi r}z}(k + \boldsymbol{N}_{\boldsymbol{2}_z} - 1|k) - \boldsymbol{x}_{\boldsymbol{\xi r}z}(k|k) \end{bmatrix},$$

$$\widehat{\widetilde{\boldsymbol{u}}}_{\boldsymbol{\xi r}z} \triangleq \begin{bmatrix} U_{1_r}(k|k) - U_{1_r}(k-1|k) \\ \vdots \\ U_{1_r}(k + \boldsymbol{N}_{\boldsymbol{u}_z} - 1|k) - U_{1_r}(k-1|k) \end{bmatrix}$$

where $\boldsymbol{N}_{\boldsymbol{u}_z}$ is the control horizon.

Minimizing the Eq. (38) when the constraints are not considered, the control law can be obtained as:

$$\widehat{\widetilde{\boldsymbol{u}}}_{\boldsymbol{\xi}z} = \left[\boldsymbol{H}_z'\boldsymbol{Q}_z\boldsymbol{H}_z + \boldsymbol{R}_z\right]^{-1} \cdot \left[\boldsymbol{H}_z'\boldsymbol{Q}_z\left(\widehat{\boldsymbol{x}}_{\boldsymbol{\xi r}z} - \boldsymbol{P}_z\boldsymbol{x}_{\boldsymbol{\xi}z}(k)\right) + \boldsymbol{R}_z\widehat{\widetilde{\boldsymbol{u}}}_{\boldsymbol{\xi r}z}\right], \tag{40}$$

although only $\widehat{\widetilde{\boldsymbol{u}}}_{\boldsymbol{\xi}z}(k|k)$ is needed at each instant k (Camacho & Bordons, 1998). Therefore, the following control signal is applied to the helicopter: $U_1(k) = \widehat{\widetilde{\boldsymbol{u}}}_{\boldsymbol{\xi}z}(k|k) + U_{1_r}(k)$.

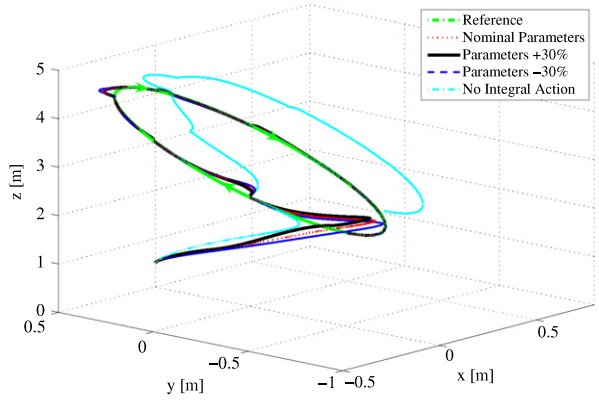

Fig. 3. Path following.

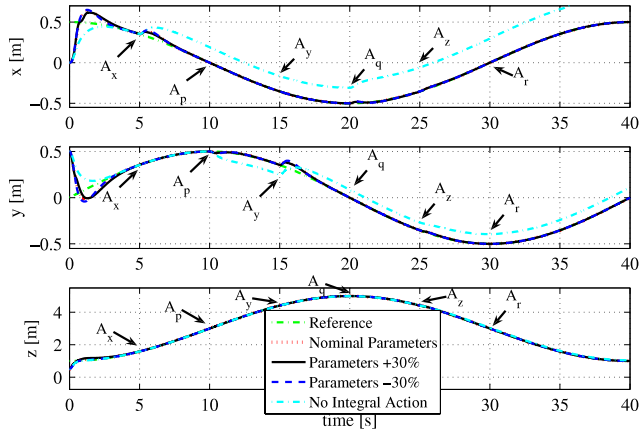

Fig. 4. Position (x, y, z).

The second control law computes the x and y motion control inputs. If the same previous procedure is carried out using the error model (35) and (37), the following control signal is obtained:

$$\widehat{\widetilde{\boldsymbol{u}}}_{\xi xy} = \left[\boldsymbol{H}'_{xy}\boldsymbol{Q}_{xy}\boldsymbol{H}_{xy} + \boldsymbol{R}_{xy}\right]^{-1} \times \left[\boldsymbol{H}'_{xy}\boldsymbol{Q}_{xy}\left(\widehat{\boldsymbol{x}}_{\xi \boldsymbol{r} xy} - \boldsymbol{P}_{xy}\boldsymbol{x}_{\xi xy}(k)\right) + \boldsymbol{R}_{xy}\widehat{\widetilde{\boldsymbol{u}}}_{\xi \boldsymbol{r} xy}\right], \tag{41}$$

where $\widehat{\widetilde{\boldsymbol{u}}}_{\xi xy}(k|k) = [\tilde{u}_x(k|k) \quad \tilde{u}_y(k|k)]'$, and

$$\boldsymbol{u}_{\xi xy}(k) = \boldsymbol{u}_{\xi \boldsymbol{r} xy}(k) + \widehat{\widetilde{\boldsymbol{u}}}_{\xi xy}(k|k). \tag{42}$$

The reference vectors of the error states, $\widehat{\boldsymbol{x}}_{\xi \boldsymbol{r} xy}$, and the error control inputs, $\widehat{\widetilde{\boldsymbol{u}}}_{\xi \boldsymbol{r} xy}$, are obtained by the same way as the one of the height controller case.

Taking into account that the required virtual inputs, $\boldsymbol{u}_{\xi xy}(k)$, to follow the path reference in the xy plane have been obtained, the necessary values of ϕ and θ could be computed by (31). At this point, it should be noted that Eq. (31) constitutes a definition of the system to be controlled. Therefore, these values cannot be set directly since these angles are two of the outputs of the rotational subsystems; being the nonlinear $\mathcal{H}_\infty$ inner loop in charge of carrying out this task.

In consequence, a desired virtual directions vector, $\bar{\boldsymbol{u}}_{\xi xy}(k) = [\bar{u}_x \; \bar{u}_y]'$, must be defined in the same sense of Eq. (31) as follows:

$$\begin{aligned} \bar{u}_x(t) &= \cos\psi(t)\sin\theta_r(t)\cos\phi_r(t) + \sin\psi(t)\sin\phi_r(t) \\ \bar{u}_y(t) &= \sin\psi(t)\sin\theta_r(t)\cos\phi_r(t) - \cos\psi(t)\sin\phi_r(t). \end{aligned} \tag{43}$$

Thereby, if $\boldsymbol{u}_{\xi xy}(k)$ is substituted by its desired value in Eq. (42), the following expression is obtained:

$$\begin{bmatrix} \bar{u}_x(k) \\ \bar{u}_y(k) \end{bmatrix} = \begin{bmatrix} \tilde{u}_x(k|k) \\ \tilde{u}_y(k|k) \end{bmatrix} + \begin{bmatrix} u_{x_r}(k) \\ u_{y_r}(k) \end{bmatrix}. \tag{44}$$

Once the desired virtual inputs have been computed, the reference of the roll and pitch angles, ϕ_r and θ_r respectively, are derived using Eq. (43). These references are necessary for the helicopter rotational loop.

6. Simulation results

The proposed control strategy has been tested by simulation in order to check the performance attained for the path following problem. Besides, simulations comparing the control structure developed in this paper with the one of Bouabdallah and Siegwart (2007) have been performed in order to show the improvement obtained with the proposed strategy. This backstepping control strategy has been chosen for the comparison analysis because it is able to present similar performance results, as well as being also able to reject sustained disturbances. Simulations have been carried out with a more accurate model, which emulates a real quadrotor helicopter, using the crossed inertia terms in the moment of inertia tensor and saturated control inputs. Moreover, the simulations have been executed considering external disturbances on the six degrees of freedom, and structural and parametric uncertainties. Taking into account that the simplified model derived in Section 2 is used just for control synthesis purposes, structural uncertainties are present because that model considers a moment of inertia tensor with only diagonal inertia terms.

The initial conditions of the helicopter are $\boldsymbol{\xi_0} = [0 \quad 0.5 \quad 0.5]'$ m and $\boldsymbol{\eta_0} = [0 \quad 0 \quad 0.5]'$ rad. The values of the model parameters used for simulations are the following: $m = 0.74$ kg, $l = 0.21$ m, $g = 9.81$ m/s^2 and $I_{xx} = I_{yy} = 0.004$ kgm^2, $I_{zz} = 0.0084$ kgm^2. An uncertainty of $\pm 30\%$ in the elements of the mass and inertia matrix has been considered in the simulations.

Assuming that the quadrotor helicopter needs, under ideal conditions, a thrust value of about $U_1 \approx 7.23$ N to perform hovering flight, the following persistent light gusts of wind are considered as external disturbances on the aerodynamic forces and moments: $A_x = 1$ N at $t = 5$ s; $A_p = 1$ Nm at $t = 10$ s; and $A_y = 1$ N at $t = 15$ s; $A_q = 1$ Nm at $t = 20$ s; $A_z = 1$ Nm at $t = 25$ s; and $A_r = 1$ Nm at $t = 30$ s.

The E-SSPC parameters were adjusted as follows:

$$\begin{aligned} &\boldsymbol{N}_{2_z} = \boldsymbol{N}_{\boldsymbol{u}_z} = 3\boldsymbol{I}_{n_z}, \qquad \boldsymbol{Q}_z = \mathrm{diag}(1, 0.8, 10), \qquad R_z = 0.05 \\ &\boldsymbol{N}_{2_{xy}} = 10\boldsymbol{I}_{n_{xy}}, \qquad \boldsymbol{N}_{\boldsymbol{u}_{xy}} = 10\boldsymbol{I}_{n_{xy}}, \\ &\boldsymbol{Q}_{xy} = \mathrm{diag}(26, 35, 20, 26, 35, 20), \qquad \boldsymbol{R}_{xy} = \mathrm{diag}(75, 75). \end{aligned}$$

The nonlinear $\mathcal{H}_\infty$ controller gains were tuned with the following values: $\omega_1 = 0.1$, $\omega_2 = 3$, $\omega_3 = 9$ and $\omega_u = 1.5$.

The first reference path used is a circle evolving in the $\Re^3$ Cartesian space defined by:

$$x_r = \frac{1}{2}\cos\left(\frac{\pi t}{20}\right) \text{ m}, \quad y_r = \frac{1}{2}\sin\left(\frac{\pi t}{20}\right) \text{ m},$$

$$z_r = 3 - 2\cos\left(\frac{\pi t}{20}\right) \text{ m}, \quad \psi_r = 0 \text{ rad}.$$

Figs. 3–7 show the simulation results of the path following of this reference trajectory. The way in which the helicopter follows the reference for different vehicle parameters is presented in Figs. 3 (in the 3D space) and 4. Besides, some marks have been included in this last figure, indicating the moments the disturbances have been applied.

It can be seen how, starting from an initial position far from the reference, the proposed control strategy is able to make the vehicle follow the reference trajectory. In addition, the vehicle trajectory in the case of no integral action is considered in the control strategy, is also presented in this figure. It can be clearly observed that, in

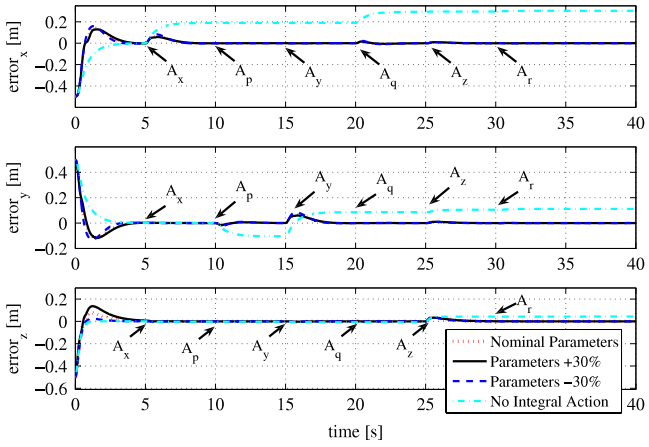

Fig. 5. Position error (x, y, z).

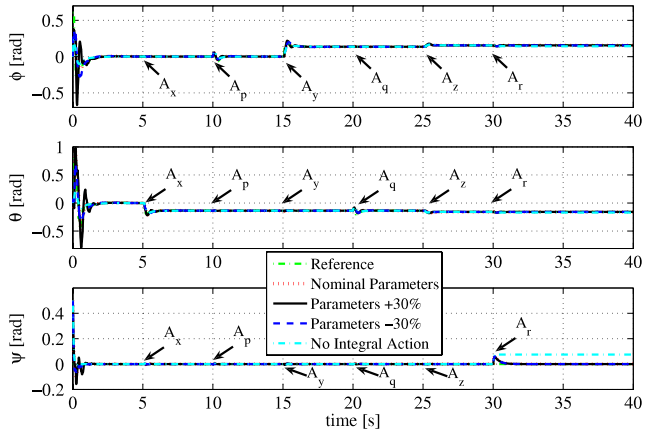

Fig. 6. Orientation (ϕ, θ, ψ).

this last case, the vehicle leaves the trajectory of reference when a disturbance is introduced, and it never reaches the reference again.

Fig. 5 shows the translational coordinates errors. It can be seen that null steady-state error is achieved for all coordinates, even if structural uncertainty is considered in the vehicle. Besides, this figure also shows that a null steady-state error is not obtained in the case of no integral action is included in the controller synthesis.

The way the inner nonlinear $\mathcal{H}_\infty$ controller makes the vehicle track its rotational references is presented in Figs. 6 and 7. It can be observed how highly-coupled the system is, since each degree of freedom is affected by the disturbances applied to the whole helicopter. The first figure shows how the references generated by the (E-SSPC) translational controller, i.e. ϕ_r and θ_r, varies in its attainment of an appropriate performance in the translational loop. On the other hand, Fig. 7 corroborates the fact that null steady-state error is also achieved for the inner loop variables, unless in the case of no integral action is considered by the inner loop controller.

A second simulation collection has been carried out with a reference trajectory made up of a set of several kinds of stretches, starting from $x_{r_0} = 0.5$ m, $y_{r_0} = 0.0$ m, $z_{r_0} = 1.0$ m and $\psi_{r_0} = 0$ rad. In these simulations, results attained by the integral MPC with the nonlinear $\mathcal{H}_\infty$ control strategy are compared with the ones achieved by the integral backstepping controller proposed by Bouabdallah and Siegwart (2007). The parameters for both control structures have been synthesized to obtain a smooth reference tracking, with a quick disturbance rejection and a minimum transient error. The simulation results are depicted in Figs. 8–11.

These figures show that both control strategies present a robust path following when abrupt changes of references and sustained disturbances are applied to the system.

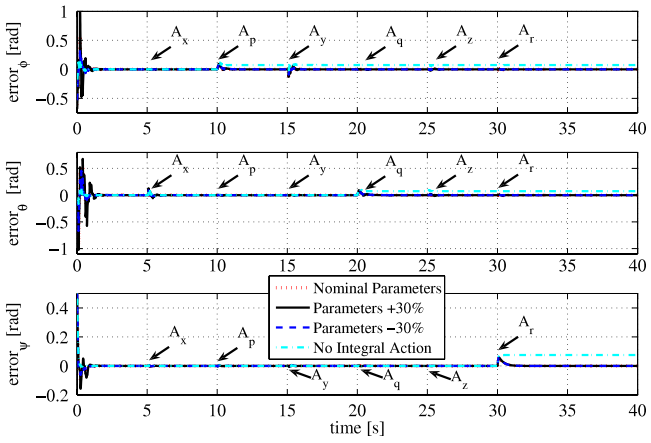

Fig. 7. Orientation error (ϕ, θ, ψ).

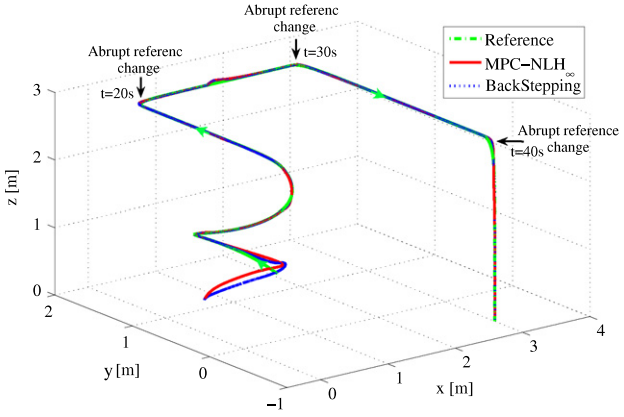

Fig. 8. Path following.

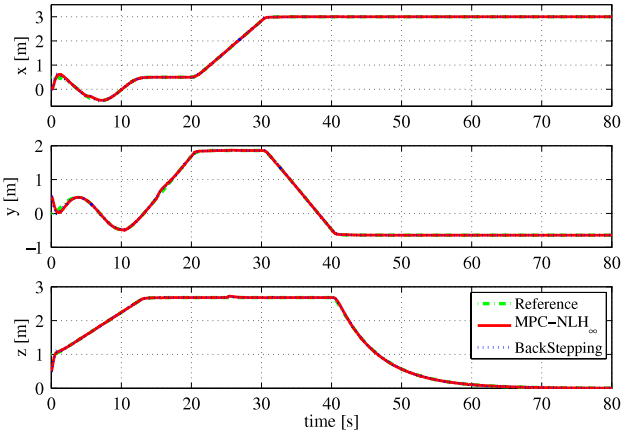

Fig. 9. Position (x, y, z).

In order to make a quantitative comparison of the results attained by these two control strategies, some performance indexes have been computed.

On one hand, the Integral Square Error (ISE) performance indexes obtained from the simulation results are presented in Table 1. It can be observed that the performance is improved by the Integral MPC/Nonlinear $\mathcal{H}_\infty$ control strategy for all states ($x \downarrow$ 30.05%, $y \downarrow$ 25.47%, $z \downarrow$ 40.62%, $\phi \downarrow$ 76.13%, $\theta \downarrow$ 40.66% and $\psi \downarrow$ 11.48%).

Although higher overshoots in the x and y error responses are presented at the beginning of the trajectory (see Fig. 10), the accumulated error along the path is lesser than the error achieved by the backstepping controller.

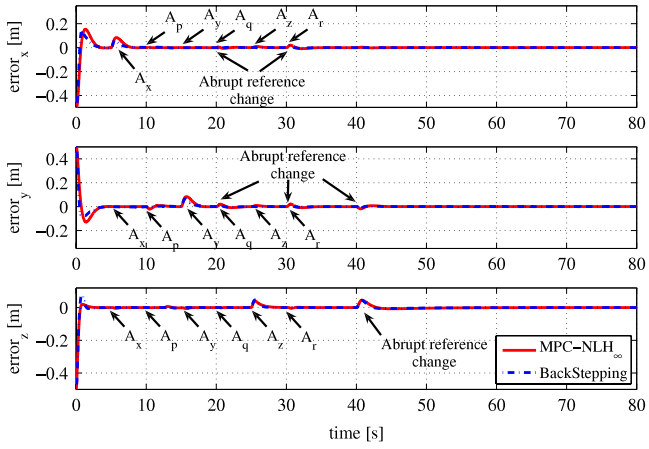

Fig. 10. Position error (x, y, z).

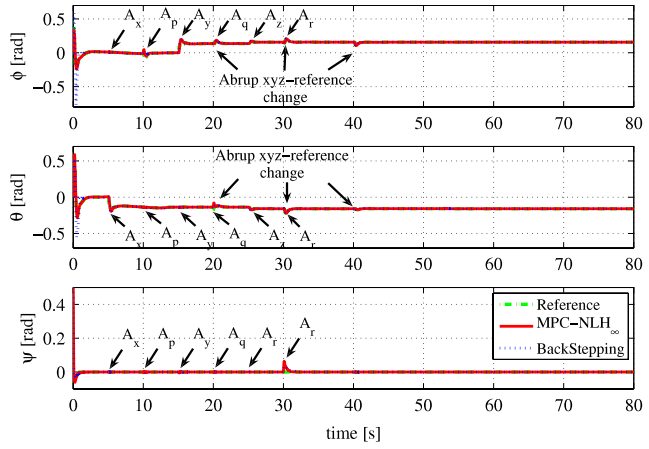

Fig. 11. Orientation (ϕ, θ, ψ).

Table 1
ISE index performance analysis.

States	MPC + NL $\mathcal{H}_\infty$	BackStepping
x	18.2883	26.1467
y	16.4420	22.0603
z	11.2947	19.0209
ϕ	4.6388	19.4346
θ	4.7846	8.0633
ψ	4.6225	5.2219

On the other hand, the Integral Absolute Derivative control signal (IADU) index has been computed for all control signals in both control strategy (depicted in Fig. 12). This performance index is very appropriate to check the control signals' smoothness. As presented in Fig. 12, the integral MPC/Nonlinear $\mathcal{H}_\infty$ control strategy generates smoother input control signals than the other strategy, underlining the quality and the feasibility of the proposed control structure. The results obtained from the simulation are presented in Table 2. It can be seen that the smoothness is also improved by the Integral MPC/Nonlinear $\mathcal{H}_\infty$ control strategy for all control signals ($U_1 \downarrow$ 15.26%, $\tau_{\phi_a} \downarrow$ 68.02%, $\tau_{\theta_a} \downarrow$ 70.32%, and $\tau_{\psi_a} \downarrow$ 56.63%).

7. Conclusions

An integral predictive and robust nonlinear $\mathcal{H}_\infty$ control strategy to solve the path following problem for a quadrotor helicopter has been presented in this paper. The proposed control strategy has been designed under consideration of external disturbances acting on all degrees of freedom. The control strategy has been split into two stages.

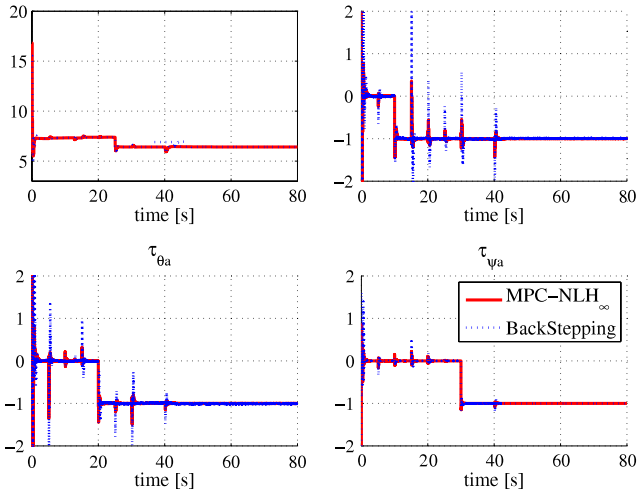

Fig. 12. Control inputs $(U_1, \tau_{\phi_a}, \tau_{\theta_a}, \tau_{\psi_a})$.

Table 2
IADU index performance analysis.

Control signals	MPC + NL $\mathcal{H}_\infty$	BackStepping
U_1	17.6692	20.8502
τ_{ϕ_a}	63.9550	199.9717
τ_{θ_a}	65.4172	220.3820
τ_{ψ_a}	18.7141	43.1515

On one hand, a state-space predictive controller for the translational movements has been proposed for the outer loop, which achieves a good and smooth performance in the reference tracking. Besides, to reject sustained disturbances affecting the translational motion, the integral of the position error has been considered in the error model used by the predictive controller.

On the other hand, a robust control for the helicopter stabilization based on nonlinear $\mathcal{H}_\infty$ theory has been designed for the inner loop. This controller is also able to reject sustained disturbances due to the use of the integral action in the state vector.

The robustness, the smoothness and the predictive feature of the proposed control strategy have been corroborated by simulations, where parametric and structural uncertainties, and unmodelled dynamics, besides sustained disturbances, have been taken into account.

The results have presented an excellent tracking of the several classes of trajectories, and have illustrated the robust performance provided by the nonlinear $\mathcal{H}_\infty$ inner controller in the case of parametric uncertainties in the mass and inertia terms. Moreover, the use of integral action in the inner and outer loop controllers has provided the capability to deal with sustained disturbances when all degrees of freedom are affected by this kind of perturbation in different moments of time.

To show the improvements achieved by the proposed control strategy, a comparative analysis between the proposed control strategy and other recent controller has been carried out by means of the ISE and IADU performance indexes.

Finally, future work will involve the implementation of this control strategy in a real quadrotor helicopter. A new vehicle is being built, which will include an appropriate control hardware to compute control signal. Since explicit control laws have been synthesized, no problem is expected regarding sampling times.

Acknowledgements

The authors would like to thank CICYT for funding this work under grants DPI2006-07338 and DPI2007-64697.

References

Bouabdallah, S., Murrieri, P., & Siegwart, R. (2004). Design and control of an indoor micro quadrotor. In *Proc. IEEE Int. conf. on rob. and automat., Vol. 5*, New Orleans, USA (pp. 4393–4398).

Bouabdallah, S., Noth, A., & Siegwart, R. (2004). PID vs LQ control techniques applied to an indoor micro quadrotor. *Proc. IEEE int. conf. on intelligent robots and systems, Vol. 3*, Sendai, Japan (pp. 2451–2456).

Bouabdallah, S., & Siegwart, R. (2007). Full control of a quadrotor. In *Proc. of the intelligent robots and systems. IROS 2007*, San Diego, USA (pp. 153–158).

Camacho, E., & Bordons, C. (1998). *Model predictive control*. New York: Springer-Verlag.

Castillo, P., Lozano, R., & Dzul, A. (2005a). Stabilization of a mini rotorcraft with four rotors. *IEEE Control Systems Magazine*, 45–55.

Castillo, P., Lozano, R., & Dzul, A. E. (2005b). *Modelling and control of mini-flying machines*. London, UK: Springer-Verlag.

Chen, M., & Huzmezan, M. (2003). A combined MBPC/2DOF $\mathcal{H}_\infty$ controller for a quad rotor UAV. In *Proc. AIAA guidance, navigation, and control conference and exhibit*, TX, USA.

Craig, J. J. (1989). *Introduction to robotics — Mechanics and control* (2nd edn). USA: Addison-Wesley Publishing Company, Inc.

Fantoni, I., & Lozano, R. (2002). *Non-linear control for underactuated mechanical systems*. London: Springer-Verlag.

Feng, W., & Postlethwaite, I. (1994). Robust nonlinear H_∞/adaptive control of robot manipulator motion. *Proceedings of the Institution Mechanical Engineers*, *208*, 221–230.

Guenard, N., Hamel, T., & Mahony, R. (2008). A practical visual servo control for an unmanned aerial vehicle. *Robotics, IEEE Transactions on [see also Robotics and Automation, IEEE Transactions on]*, *24*(2), 331–340.

Kühne, F., Lages, W. F., & Gomes Da Silva, J. M. (2005). Point stabilization of mobile robots with nonlinear model predictive control. In *Proc. of the IEEE mechatronics and robotics, Vol. 3*, Niagara Falls, Canada (pp. 1163–1168).

Madani, T., & Benallegue, A. (2007). Sliding mode observer and backstepping control for a quadrotor unmanned aerial vehicles. In *Proc. of American control conference, 2007. ACC '07*, NY, USA (pp. 5887–5892).

Mistler, V., Benallegue, A., & M'Sirdi, N.K. (2001). Exact linearization and noninteracting control of a 4 rotors helicopter via dynamic feedback. In *Proc. IEEE int. workshop on robot and human inter. communic.*

Mokhtari, A., Benallegue, A., & Daachi, B. (2006). Robust feedback linearization and $\mathcal{G}H_\infty$ controller for a quadrotor unmanned aerial vehicle. *Journal of Electrical Engineering*, *57*(1), 20–27.

Mokhtari, A., Benallegue, A., & Orlov, Y. (2006). Exact linearization and sliding mode observer for a quadrotor unmanned aerial vehicle. *International Journal of Robotics and Automation*, *21*(1), 39–49.

Olfati-Saber, R. (2001). Nonlinear control of underactuated mechanical systems with application to robotics and aerospace vehicles. *Ph.D. thesis*. Massachusetts Institute of Technology.

Ortega, M. G., Vargas, M., Vivas, C., & Rubio, F. R. (2005). Robustness improvement of a nonlinear H_∞ controller for robot manipulators via saturation functions. *Journal of Robotic Systems*, *22*(8), 421–437.

Raffo, G. V., Gomes, G. K., Normey-Rico, J. E., Kelber, C. R., & Becker, L. B. (2009). A predictive controller for autonomous vehicle path tracking. *IEEE Transactions on Intelligent Transportation Systems*, *10*(1), 92–102.

Raffo, G. V., Ortega, M. G., & Rubio, F. R. (2008). Backstepping/nonlinear $\mathcal{H}_\infty$ control for path tracking of a quadrotor unmanned aerial vehicle. In *Proc. of the 2008 American control conference — ACC2008*, Seattle, USA (pp. 3356–3361).

Rossiter, J. A. (2003). *Model-based predictive control: A practical approach*. New York: CRC Press.

Sun, S. (2005). Designing Approach on trajectory-tracking control of mobile robot. *Robotics and Computer-Integrated Manufacturing*, *21*(1), 81–85.

Van der Schaft, A. (1992). L_2-gain analysis of nonlinear systems and nonlinear state feedback control. *Institute of Electrical and Electronics Engineers. Transactions on Automatic Control*, *37*(6), 770–784.

Van der Schaft, A. (2000). *L_2-gain and passivity techniques in nonlinear control*. New York: Springer-Verlag, p. 249.

Zemalache, K. M., Beji, L., & Maaref, H. (2007). Two inertial models of x4-flyers dynamics, motion planning and control. *Integrated Computer-Aided Engineering*, *14*(2), 107–119.

Guilherme V. Raffo was born in Porto Alegre, Brazil, in 1979. He received the B.Sc. degree in automation and control engineering from Pontifical Catholic University of Rio Grande do Sul – PUC-RS, Brazil, in 2002, his specialist degree in industrial automation from Federal University of Rio Grande do Sul (UFRGS), Brazil, in 2003 and his M.Sc. degree in electrical engineering from Federal University of Santa Catarina (UFSC), Brazil, in 2005. He is currently working toward the Ph.D. degree at University of Seville, Spain, in robust control and $\mathcal{H}_\infty$ theory applied to UAV.

From August to December 2008 he had a research stay at the University of Leicester, England, with the Control and Instrumentation Research Group working in air traffic control, as part of his Ph.D. His current research interests include robust control, $\mathcal{H}_\infty$ theory, predictive control and robotic systems.

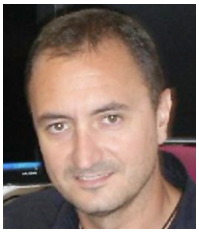

Manuel G. Ortega was born in Jaén, Spain, in 1969. He received the M.Sc. degree in Industrial Electrical Engineering, and the Ph.D. degree in System Engineering and Automation (with doctoral award), both from the University of Seville, Spain, in 1995 and 2001, respectively. From 1996 to 2004, he was a Research Assistant under several grants and was an Assistant Professor at the Department of Systems Engineering and Automation of the University of Seville. Since 2004, he has been an Associate Professor at the same Department. Dr. Ortega has worked in various research and development projects in cooperation with industry. He is the author or co-author of more than 35 publications including journal papers, book chapters, and conference proceedings. His current research interests include robust control, $\mathcal{H}_\infty$ control theory, nonlinear control systems, robotics, and process control.

Francisco R. Rubio received the Industrial Electrical Engineering degree and Doctorate from the Escuela Técnica Superior de Ingenieros Industriales de Sevilla in 1981 and 1985, respectively. He received the CITEMA award for the best work on automation by a young engineer in 1980. He is a Professor in the Department of Systems Engineering and Automatic Control of the University of Seville. He has worked on various research and development projects in cooperation with industry. His current interests are in the areas of adaptive control, robust process control, nonlinear control systems and robotics. He has written two books: Advanced Control of Solar Plants published by Springer-Verlag and Control Adaptativo y Robusto published by Seville University. He has authored and co-authored more than 150 technical papers published in international journals and conference proceedings.